Polynomial regression of multiple sensing variables for high-performance smartphone colorimeter

SAPTAMI RANI,[1,*] PROTIK CHANDRA BISWAS,[1] MD ARAFAT HOSSAIN,[1] MD RAFIQUL ISLAM,[1] AND JOHN CANNING [2]

[1]*Department of Electrical and Electronic Engineering, Khulna University of Engineering & Technology, Khulna 9203, Bangladesh*
[2]*Interdisciplinary Photonics Laboratories, School of Electrical and Data Engineering, The University of Technology Sydney, NSW 2007, Australia*
* *rani2003752@stud.kuet.ac.bd*

Abstract: A robust and adaptive smartphone-based colorimetric sensing platform is reported. It utilizes multiple regression analysis to address nonlinear concurrent variations of multiple sensing variables. The instrument can perform colorimetric measurement with improved accuracy over a wide range where both color and intensity information of a colorimetric signal varies independently often simultaneously. The instrument utilizes the smartphone in-built flash LED (λ = 400-700 nm) to illuminate the test sample and the phone's CMOS camera as a detector, collecting and digitizing the reflected light from that sample. 3D printing technology is used to fabricate a specially designed optical enclosure that performs as a diffuser, neutral density filter, and reflector to ensure constant and uniform illumination of the sensing platform. Thus, an ultra-low-cost (< 3 USD) portable smartphone-based colorimetric diagnostic system becomes feasible along with an easy-to-use customized android app adaptable for multi-analyte assays. The performance of the colorimetric measurement system is validated by: (a) monitoring the concentration of a laser dye, (b) measuring the pH of drinking water, and (c) quantifying the chlorine concentration of shrimp ponds.

1. Introduction

Smart sensing and measurements are underpinning the Internet-of-Things (IoT) typically located at the network end face where there is a point-of-need [1-5]. These measurements usually rely on colorimetric detection that is simply based on digitizing color information of a sample using a portable camera device. The color information is quantified and used to assess the physical and chemical characteristics of the target analyte. Recent advances in complementary metal-oxide-semiconductor (CMOS) technologies coated with selective partial red, green and blue (RGB) filters and their interfacing electronics have enabled compact and low-cost colorimetric detection with portable smart devices such as smartphone, digital cameras, and more [6-9]. These can offer an equivalent performance against high-end photodetectors and arrays used in benchtop instruments. In particular, the smartphone-based colorimeter can offer easy-to-use, fast measurement, remote control, low-cost and data management.

Colorimetry has been used widely for smartphone-based measurements because it is simple and offers excellent color detection [10-15]. Colorimetry is not a spectral measurement approach [16-18] but rather a color analysis of the combinations of integrated emission bands within the three-color spectral bands as filtered to the CMOS detector by distributed RGB pixel filters. In a simple smartphone colorimeter, sensing parameters are typically extracted by recording the intensity of the RGB color channels of the CMOS camera and calibrating them against the response recorded by a standard colorimeter [10, 11, 19, 20].

However, the technique is sensitive to variations in ambient illumination often made worse by software adjustments. There are also non-monotonical changes in RGB responses in different colors and intensity that happen with the variation of analytes which are simply difficult to determine using the linear response within a single-color channel [19, 21]. The first part has been addressed partially by introducing 3D-printable custom-designed enclosures that mainly aim to block the unwanted stray illumination reaching the camera detector [4, 14, 22]. The addition of a reference to the measurement also helps to reduce the unexpected biasing of results from ambient variations thus allowing measurements by direct camera imaging [23, 24]. Nevertheless, the later part introduces severe problems in colorimetric detection particularly that associated with an independent or concurrent variation of color and intensity. Here, intensity means the quantity of visible light reflected by or transmitted through the sample solution and captured on the CMOS detector for only three specific color bands that are defined by the *R*, *G*, and *B* color filters of the detector and quantified to fit within a number between 0 to 255 (8-bits number). The variation of intensity and color with samples can be correlated using color models such as HSV that show relatively better performance and stability as compared to the primary RGB model [25, 26]. HSV is a cylindrical coordinate representation of an RGB color model where the color change information is defined by the hue (*H*) and the intensity parameter is represented by the value (*V*) and saturation (*S*) information of the color map [25-29]. The change of *H* information is reported with a monotonic change of sensing parameters such as pH, glucose, protein in bio-samples [30, 31]. Other applications show a sharp variation of *S* parameters with analytes at a particular *H*-value [32]. It should be noted that each of the above techniques demonstrates a significant contribution to addressing the issues of traditional CMOS-based colorimetric sensing. However, the dependence on a single sensing variable reduces the detection sensitivity and the range of detection. The use of both variables was partially utilized in a smartphone colorimeter for sensing multi-analytes where color and intensity responsive analytes are separated as *H*-type and *S*-type respectively [26]. Their actual measurement, however, considers a single sensing parameter. To enable an accurate, highly sensitive, and widely applicable colorimetric detection, image processing requires an adaptive analysis that combines both concurrent and differential variations of multiple sensing variables (color and intensity) [33].

In this work, a generalized and adaptive colorimetric sensing platform is developed using multiple regression analysis of the nonlinear concurrent variations of color and intensity. The underlying idea is based on the increasing and decreasing optical sensing parameters with associated weight vectors that produce a proportional output signal. A 3D-printed enclosure is designed to hold the sample cuvette attached to the smartphone camera, enabling it to perform measurements in fields. The performance of the colorimeter considering both HSV and RGB color model is analyzed and validated with a field demonstrated colorimetric quantification in three different applications: (1) concentration quantification of a laser dye, (2) pH measurement of drinking water, and (3) chlorine (Cl) concentration quantification of shrimp ponds.

2. Smartphone colorimeter: materials and methods

2.1 Optical layout

The optical layout of the smartphone colorimeter is shown in Fig. 1(a). It mainly consists of a smartphone attachment holding a sample cuvette at a fixed distance (d = 3.5 cm) in front of the rear-facing camera unit. The colorimeter utilizes the in-built flash LED (λ = 400 ~ 700 nm) for illuminating the sample whereas the rear-facing CMOS camera is used for detecting the colors. For optimal imaging of the camera, a customized pinhole and diffuser setup are used that allow the flash LED to illuminate the sample uniformly. The emission of the LED propagates from the source to the sample as well as when it reflects back to the camera from the attachment surface placed at the other side of the sample cuvette wall. The use of back

reflection doubles the optical path length, improving the colorimeter detection sensitivity. Additionally, the 3D printed enclosure improves the optical signal-to-noise ratio by rejecting all ambient illumination reaching the camera.

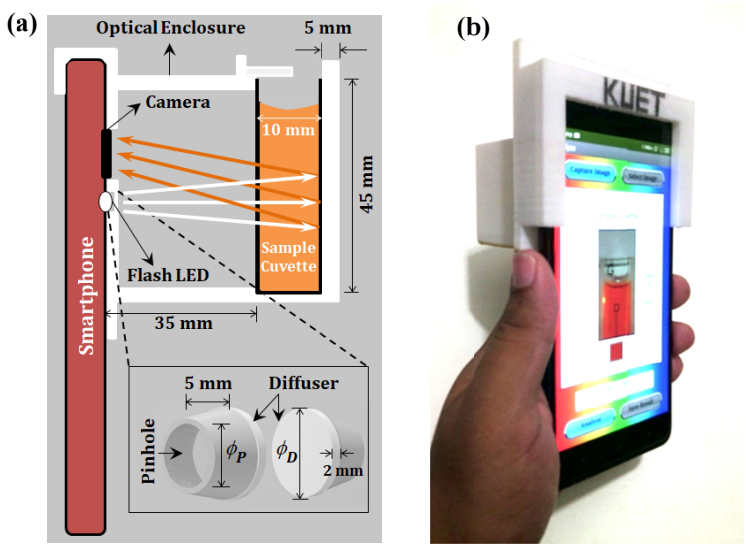

Fig. 1. Adaptive smartphone colorimeter: (a) the optical layout; inset shows 3D printed customized pinhole and diffuser setup fabricated with the optical enclosure by utilizing white PLA filament, and (b) the 3D printed final device installed on an android smartphone.

2.2 3D design and fabrication

The 3D design of the smartphone colorimeter enclosure is modeled in AutoCAD and fabricated on a desktop FDM printer using white polylactic acid (PLA) plastic. The design is made compatible with a Xiaomi Redmi Note 4 smartphone (13 MP rear-facing camera, 1080×1920 pixels display resolution) although it can be fitted to any other smartphone camera with a simple modification of the 3D design. The optical enclosure contains a pinhole (ϕ_P = 4 mm) and a circular slot (ϕ_C = 10 mm) that fit the optical source and camera detector respectively.

A 3D-printed white PLA thin film (t_D = 2 mm) is placed vertically in front of the pinhole which diffuses the bright emission of the flash LED. It also acts as a neutral density filter for optimum imaging performance. Whilst the printing parameters, such as layer thickness and infill material density, influence the diffusing and filtering performance of the PLA filter, the layer thickness of 0.15 mm and infill density of 20% are found suitable for the smartphone colorimeter. Considering these printing parameters and design specifications, 3D fabrication takes about 4.5 hours and cost of PLA filament is 2.9 USD. The white PLA surfaces of the enclosure with 3D-printed micro-grains also help diffuse light over the sample uniformly without the need for expensive optics. A sliding shutter at the top of the sample chamber provides user access to the sample. By employing the 3D-printed smartphone attachment with all customized optics, the entire colorimeter is made robust, inexpensive (< 3 USD), compact and lightweight (70 gm) for field portable operation.

2.3 Polynomial regression-based colorimetric detection

In a simple colorimetric analysis, the information of a measured parameter or variable (e.g. chemical composition, biological species, and so on) is typically determined by imaging the sample using a camera and digitizing the image color parameters that are expected to reflect

the changes in measurement. In conventional smartphone colorimeters, simple linear or nonlinear regression techniques are used to quantify a measurement variable based on a single explanatory variable extracted by utilizing single channel information of HSV color model [2, 3, 7, 12]. The RGB values of the digitized image are also directly used to calculate a single explanatory variable (color ratio or an average of the RGB values) for simple regression analysis in many smartphone-based analytical measurements [4, 34]. But, a well-defined study variable of the sample is highly correlated with all the *H*, *S*, and *V* channels information linearly or nonlinearly. In RGB color model, this change is associated with *R*, *G*, and *B* information. In order to include the effects of all possible explanatory variables, we introduce a multiple regression analysis that considers the nonlinear concurrent variations of *H*, *S*, and *V* information or *R*, *G*, and *B* information. The *R*, *G*, and *B* channel information are extracted from the color parameters captured by the smartphone camera that forms an equivalent RGB color image on the screen. To extract the *H*, *S*, and *V* values, the primary RGB color is transformed into equivalent cylindrical coordinates by using the Eqs. (1)-(6). In HSV color model, color (*H*) and intensity (*S* and *V*) information is decoupled. But these information are complexly composited among the three channels of the RGB color model [26, 35].

$$Max_{RGB} = \max\left(\frac{R}{255}, \frac{G}{255}, \frac{B}{255}\right) \tag{1}$$

$$Min_{RGB} = \min\left(\frac{R}{255}, \frac{G}{255}, \frac{B}{255}\right) \tag{2}$$

$$\Delta = Max_{RGB} - Min_{RGB} \tag{3}$$

$$H = \begin{cases} 0^\circ & \Delta = 0 \\ \left(\frac{R-B}{\Delta \times 255}\right) \times 60^\circ & Max_{RGB} = \frac{R}{255} \\ \left(\frac{B-R}{\Delta \times 255} + 2\right) \times 60^\circ & Max_{RGB} = \frac{G}{255} \\ \left(\frac{R-G}{\Delta \times 255} + 4\right) \times 60^\circ & Max_{RGB} = \frac{B}{255} \end{cases} \tag{4}$$

$$S = \begin{cases} 0 & Max_{RGB} = 0 \\ \frac{\Delta}{Max_{RGB}} \times 100\% & Max_{RGB} \neq 0 \end{cases} \tag{5}$$

$$V = \left(Max_{RGB} \times 100\%\right) \tag{6}$$

Polynomial regression, a technique of multiple linear regression analysis [36] is then applied to formulate the generalized equation for the dependent study variable *P* being measured by considering the independent explanatory variables *X*, *Y*, and *Z* associated with the concurrent nonlinear variation of color and intensity. Explanatory variables *X*, *Y*, and *Z* have to be considered as *H*, *S* and *V* values for the HSV model and as *R*, *G* and *B* channel information for the RGB model. The study variable is related to explanatory variables through regression coefficient matrices denoted as [a_i] and [b_{ij}] in a second-order polynomial expressed by Eq. (7). In Eq. (7), [a_i] is the matrix of linear effect parameters and [b_{ij}] is the matrix of quadratic and second order interaction effect parameters [36]. In order to define Eq. (7) for a specific application, the least squares method is applied that estimates the regression coefficients from an initial known set of *P* and *X*, *Y*, *Z* values. The final equation with known coefficient can be applied as a calibration tool to calculate subsequent unknown values of *P*

that consider any single or concurrent variation of color and intensity. To apply the equation for a different application, the coefficient will be re-estimated:

$$[P]=[a_0]+[a_1 \quad a_2 \quad a_3]\begin{bmatrix}X\\Y\\Z\end{bmatrix}+[X \quad Y \quad Z]\begin{bmatrix}b_{11} & b_{12} & b_{13}\\ b_{21} & b_{22} & b_{23}\\ b_{31} & b_{32} & b_{33}\end{bmatrix}\begin{bmatrix}X\\Y\\Z\end{bmatrix} \tag{7}$$

2.4 Colorimetric smartphone app

A custom-designed smartphone app is developed on the Android platform to measure an analyte using multiple regression-based colorimetric analysis. The app allows the user to select task options from the menu screen as shown in Fig. 2(a). This includes taking a device-specific calibration, measurement of an unknown sample, and sharing results with other devices. Color information of the test sample is digitized through image capture by utilizing the smartphone CMOS camera detector. On the captured image, a (10 × 10) pixel array is selected as region-of-interest (ROI) to extract the RGB values, depicted in Fig. 2(b). During calibration and field measurements, the ROI is maintained constant by the software program and thus any possibility of nonuniform illumination in the optical enclosure is neutralized from the measurement. The average RGB values of these pixels are transformed into the HSV color domain. The resultant *H*, *S*, and *V* parameters are incorporated into the calibration equation formulated for the selected analyte. The test results of the colorimetric assessment can be saved to the smartphone internal storage for further analysis and sharing with other devices, or sent to a central server to facilitate a wider, smart sensor network. This app also facilitates the incorporation of new colorimetric tests for different analytes in conjunction with the existing tests. Moreover, recalibration of the existing colorimetric tests is feasible for different limits of detection. For each calibration time, the regression coefficient matrices of the generalized calibration equation are re-estimated according to the color information of the standard samples of the specified analyte through multiple regression analysis.

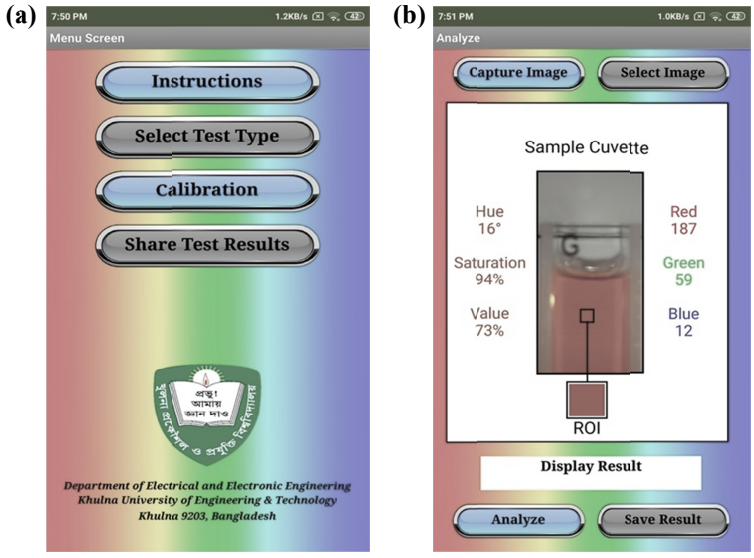

Fig. 2. Custom-developed smartphone colorimeter app. Screenshot images of (a) menu screen, and (b) analyze screen.

2.5 Calibration

The calibration of the smartphone colorimeter for a specific application enables the instrument to determine the regression coefficients in Eq. (7) for a specific analyte using a known set of standard samples. This application-specific response will allow the user to measure an unknown sample within the detection limit of the device. In this case, the instrument has been calibrated for demonstrating its performance in measuring the concentration of a laser dye (Rhodamine B, [RhB]) and two important quality indicators of the water system (pH and chlorine, [Cl]).

In order to calibrate the device for measuring the [RhB], a total of 15 samples with [RhB] ~ 0.2 to 4.0 ppm are prepared using distilled water. Images of the samples captured by the smartphone camera are shown in Fig. 3(a). The calibration option of the smart colorimetric app processes the images to extract their primary explanatory variables H, S and V. Figure 3(b) shows the variation of H, S, and V with [RhB]. It is found that the S value changes significantly with [RhB] whereas the H and V values are almost constant over the concentration range as also indicated in their images [Fig. 3(a)]. Because only intensity information changes with respect to [RhB] variation [16]. These sets of data have been applied in the polynomial regression analysis to formulate a second-order polynomial equation on the LabFit platform. The polynomial fit of [RhB] with a determination coefficient, R^2 = 0.9957370 defines the elements of the regression coefficient matrices corresponding to H, S, and V independent variables in Eq. (7). The calibrated regression coefficient matrices are summarized in Table 1. Polynomial regression analysis based on the RGB model [Fig. 3(c)] is also performed and corresponding regression coefficient matrices are tabulated in Table 1. In this case, determination coefficient (R^2 = 0.9996446) is better than that of HSV model which implies better polynomial fits.

A similar calibration procedure needs to be applied before measuring any other analytes using the smartphone colorimeter. For example, to use the device for pH sensing in water, calibration is performed against a total of 11 standard buffer solutions of known pH ranging from pH ~ 4.0 to 9.0. The solutions are prepared using a titration of 0.1 M NaOH in standard acetate and phosphate buffer at an average temperature of T ~ 25 °C. The pH value of each buffer solution is confirmed by using a standard pH meter (Ezodo PH5011).

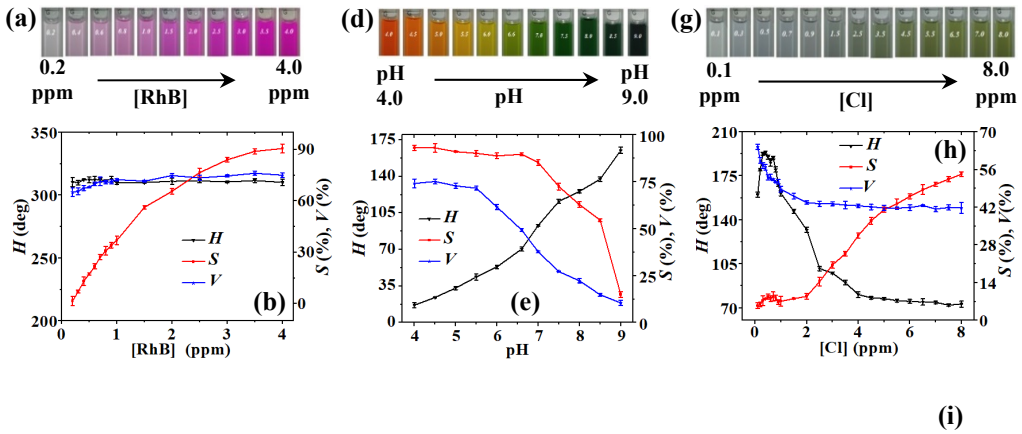

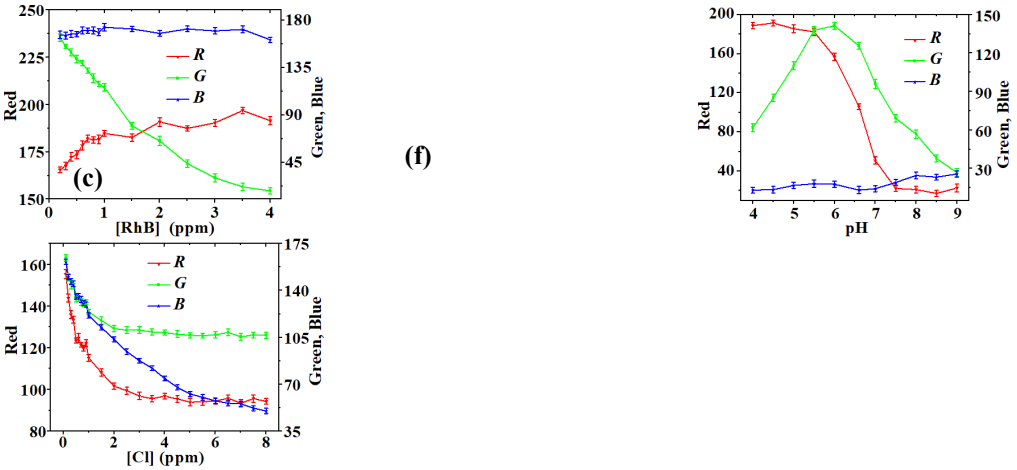

Fig. 3. Calibration of smartphone colorimeter. Standard samples for (a) [RhB] quantifier, (d) pH meter, and (g) [Cl] quantifier. Calibration curves: [RhB] quantifier based on (b) HSV & (c) RGB color model; pH meter based on (e) HSV & (f) RGB color model; [Cl] quantifier based on (h) HSV & (i) RGB color model. The error bars illustrate the relative standard deviation over three measurements.

To get a colorimetric indication of pH samples, a universal indicator solution of 0.2 ml is added to 10 ml of each buffer solution. The universal indicator changes the color differently at different values of pH as shown in Fig. 3(d). These images are analyzed to extract the regression coefficient matrices for the polynomial expression of pH for both HSV and RGB model [Table 1]. Unlike [RhB], all the explanatory variables change with pH value [Fig. 3(e) and (f)] which illustrates the nonlinear and concurrent variation of color and intensity also as indicated in Fig. 3(d).

To apply the smartphone colorimeter for measuring [Cl] content in water, it is calibrated against 24 standard samples of [Cl] ~ 0.1 to 8.0 ppm prepared by dissolving calcium hypochlorite ($Ca(ClO)_2$) in distilled water. A volume of 10 ml of each sample is added to 150 µl of potassium iodide-starch (KI-starch) solution prepared using a standard iodometric method [23]. The final solutions give a colorimetric indication of [Cl] in water as depicted by the images shown in Fig. 3(g). The sample images are analyzed following the same procedure as discussed above and the calibration curves for the HSV and RGB model are depicted in Figs. 3(h) and 3(i) respectively. Similar to the pH calibration, all possible explanatory variables are impacted and influenced the sample color [Fig. 3(g)] although the effective change of variables associated with the intensity and color information varies differently for the different rage of detection. Finally, the calibration equations are uploaded to the smartphone app to measure the [RhB], pH, and [Cl] of unknown samples.

Table 1. Estimated regression coefficient matrices for different colorimetric tests

Test name	Color model	0^{th} order coefficient matrix $[a_0]$	1^{st} order coefficient matrix $[a_1 \quad a_2 \quad a_3]$	2^{nd} order coefficient matrix $\begin{bmatrix} b_{11} & b_{12} & b_{13} \\ b_{21} & b_{22} & b_{23} \\ b_{31} & b_{32} & b_{33} \end{bmatrix}$	Determination coefficient (R^2)
[RhB]	HSV	$[10002 \cdot 3]$	$[-63.21 \quad 1.1799 \quad -5.24105]$	$\begin{bmatrix} 0.099074 & -0.004308 & 0.023537 \\ 0 & 0.000481 & 0.002004 \\ 0 & 0 & -0.014588 \end{bmatrix}$	0.9957370

quantifier	RGB	$[128.637]$	$[0.7358 \quad 0.0485 \quad -2.3386]$	$\begin{bmatrix} -0.0023 & -0.000688 & 0.001173 \\ 0 & 0.000077 & 0.000272 \\ 0 & 0 & 0.006174 \end{bmatrix}$	0.9996446
pH meter	HSV	$[2.9104]$	$[0.1522 \quad 0.1534 \quad -0.2378]$	$\begin{bmatrix} -0.000631 & -0.000997 & 0.000461 \\ 0 & -0.000826 & 0.000651 \\ 0 & 0 & 0.001041 \end{bmatrix}$	0.9999939
	RGB	$[11.3962]$	$[-0.0164 \quad -0.024 \quad -0.192]$	$\begin{bmatrix} -0.00012 & 0.000313 & -0.000001 \\ 0 & -0.000038 & -0.000349 \\ 0 & 0 & 0.005565 \end{bmatrix}$	0.9997504
[Cl] quantifier	HSV	$[8.4001]$	$[-0.0667 \quad -0.372 \quad 0.0497]$	$\begin{bmatrix} -0.00006 & 0.001786 & 0.009984 \\ 0 & 0.003657 & 0.002737 \\ 0 & 0 & -0.002452 \end{bmatrix}$	0.9987993
	RGB	$[30.525]$	$[0.8492 \quad -1.1245 \quad -0.0746]$	$\begin{bmatrix} 0.050394 & -0.08826 & -0.012616 \\ 0 & 0.041666 & 0.007396 \\ 0 & 0 & 0.002547 \end{bmatrix}$	0.9954290

3. Colorimetric measurements and performance evaluation

After calibrating the device using multiple regression analysis, it has been applied for the measurement of unknown samples that contain single or multiple variations of the explanatory variables with the target analytes. The demonstration starts with the measurements of RhB in water samples at different concentrations i.e. [RhB]. RhB is a widely available laser dye used to test and calibrate optical parameters due to its stable optical and thermal properties. To evaluate the performance of the instrument, a total of 7 samples with known [RhB] are measured using the smartphone colorimeter. The average results of three repeated measurements are compared with their actual concentrations as shown in Fig. 4(a). The deviation with the standard measurements is relatively high for HSV model based assessment (average error, $e_{\mathrm{RhB}} \sim 5.2$ %) than that of RGB model (average error, $e_{\mathrm{RhB}} \sim 1.8$ %) for same range of detection. It is noted from RGB to HSV conversion [Eqs. (1)-(6)], H variable remains constant with respect to the intensity information which is the only changing variable with [RhB]. Therefore, for [RhB] quantifier, the number of effective independent variable (N_E) of polynomial regression is reduced for HSV model ($N_E = 2$) than RGB ($N_E = 3$). So, it is concluded that, RGB color model based multiple regression analysis is more accurate than HSV for the colorimetric assessments where only the intensity information changes and color information remains constant.

The smartphone colorimeter has been used to measure the pH of drinking water from unknown sources. Amongst various parameters considered to measure water quality, pH is a particularly important indicator to determine the alkalinity or acidity of water, and standards for optimal pH values using different systems are set by the national and international health authorities. Therefore, accurate monitoring of pH is important for both biomedical and agricultural health. To measure the pH of drinking water, samples were collected from 7 different water tap located in KUET, Khulna campus, and measured using the smartphone-based colorimeter. The performance of the smartphone measurements based on HSV and RGB model was compared against sample measurements using a standard electrode-based pH meter. The smartphone measurements are in good agreement with the electrode-based

measurements for both HSV (average error, e_{pH} ~ 0.2 %) and RGB color model (average error, e_{pH} ~ 0.3 %). The HSV color model-based assessment gives slightly better performance than RGB model. For both of these color models, the number of effective independent variable is same (N_E = 3) because the dependent variable (pH) changes effectively with the independent variables of HSV and RGB model associated with color and intensity change. Inherently, independent variables of the HSV model decouple color and intensity information separately [35] and so for the colorimetric assays where both of these color information vary significantly, regressed equation based on HSV variables (R^2 = 0.9999939) fit more appropriately than RGB model (R^2 = 0.9997504) as illustrated in the Table 1.

Finally, the smartphone colorimeter has been used to measure another quality indicator of the water system, chlorine concentration, relevant to public health. Chlorine is particularly important in drinking water systems used to prevent various water-borne diseases including cholera, dysentery, and typhoid. However, the chlorine at high concentrations is toxic to many living organisms including fishes in water ecosystems. At low concentration, it stresses fishes by damaging their gills. Therefore, accurate determination of [Cl] in the water system is also important to ensure safe and healthy environments for fish and other organisms living in the water. Consequently, the smartphone colorimeter has been applied to measure [Cl] in field samples. To do this, water samples of seven shrimp farms in different locations of the Khulna region is measured using the smartphone instrument and compared against standard measurements, shown in Fig. 4(c). Shrimp farming is the main agricultural product in the region that contributes significantly to the local economy with an annual production of approximately 42,000 metric tons. Unlike a traditional [Cl] measurement, the smartphone instrument does not require sample storage and transportation to a local laboratory. It offers direct, rapid, and on-site detection of [Cl] providing an immediate opportunity for recourse by local farmers. The device with regressive color detection allows in-field determination of [Cl] with an accuracy ~ 98% and ~ 96.6% for HSV and RGB color model-based measurement respectively. Additionally, the result can be shared using the internet connectivity for further expert analysis and feedback as well as archiving for both mapping and forecasting water quality.

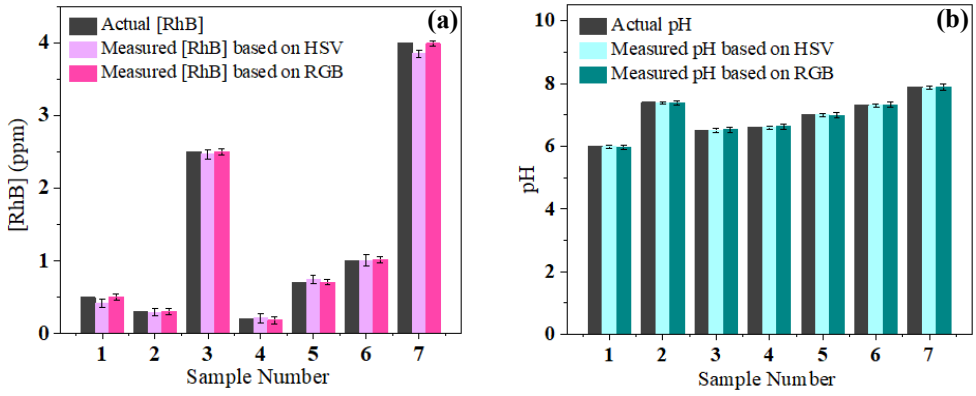

(c)

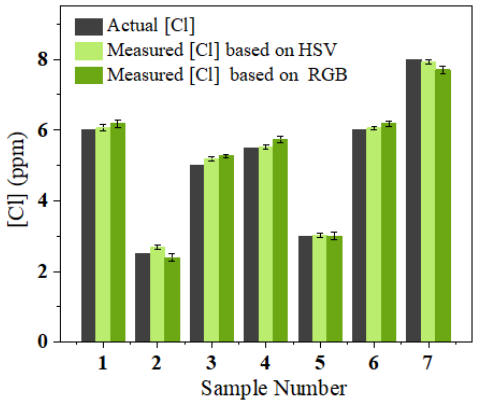

Fig. 4. Performance evaluation of the smartphone colorimeter for both HSV and RGB color model-based assessment: (a) [RhB] quantification, (b) pH measurement of drinking water, and (c) [Cl] quantification of shrimp ponds.

The effectiveness of the multiple regression-based analysis for colorimetric measurement in the above applications has been analyzed further by comparing the results against simple colorimetric measurement where a single explanatory variable (*H* or *S* or *V*) is used as a sensing parameter. For the case of colorimetric assessment of [RhB] based on single sensing parameter (*S*), measurement accuracy and range of detection are, unsurprisingly, unchanged after applying multiple regression analysis. This is because only one color and therefore one HSV parameter, *S*, is varying most significantly with [RhB]. But, in the case of pH measurement where all three-color bands change, all explanatory variables (*H*, *S*, and *V*) also change impacting the study variable pH, multiple regression generates at least a 4-fold improvement in pH measurement compared with using a color region or single explanatory variable. Similar to the pH measurement, the multiple regression also causes an expected improvement in [Cl] measurement performance where all of the explanatory variables change significantly with [Cl]. Overall, a 25-fold improvement of [Cl] detection accuracy is obtained over a single use of an HSV variable. In addition, the range of detection (ΔP) can be extended significantly by considering the impacts of both optical sensing parameters color (*H*) and intensity (*S* and *V*) in multiple regression-based analyses. For example, the detection range increases from ΔP = 3.9 (0.1 ~ 4.0) ppm to ΔP = 7.9 (0.1 ~ 8.0) ppm when all variables are considered. A similar improvement in ΔP has been achieved with the pH measurement.

Table 2. Comparison of different colorimetric assessments based on single and multiple sensing variables

Test name	Detection range	Average detection error considering multiple sensing parameters (%)		Average detection error considering a single sensing parameter (%)		
		H, *S* & *V*	*R*, *G* & *B*	*H*	*S*	*V*
[RhB]	0.2 - 4.0 (ppm)	5.2	1.8	Too high	5.2	Too high
pH	4.0 - 9.0	0.2	0.3	0.7	5.4	3.2
[Cl]	0.1 - 8.0 (ppm)	2.0	3.4	Too high	49.8	Too high

4. Conclusion

An application independent smartphone-based colorimeter has been demonstrated by using the attributes of concurrent nonlinear variation of color and intensity in a polynomial

regression-based analysis of the three-color pixel filter spectra of a CMOS camera. The technique improves the detection accuracy and the range of detection over the traditional smartphone colorimeter analysis that uses only a single sensing parameter. These improvements are primarily attributed to the nonlinear concurrent variation of multiple optical sensing variables as well as to their differential changes with the target analytes. The proof-of-concept has been demonstrated with a custom-designed 3D-printed smartphone camera attachment that allows colorimetric measurement of samples using a smart app. The instrument is demonstrated through the measurement of the laser dye concentration and two quality indicators of water systems. The present measurement approach can also be applied for the colorimetric quality detection and assessment of different foods and beverages, agricultural items, and colorimetric-based test strips using a specific calibration of the smartphone app. The results presented here are validated with the standard values of analytes that justify the detection range and the accuracy of the measurement compared to the conventional colorimetric detection technique.

Funding

This research work was supported by postgraduate research grants of Khulna University of Engineering & Technology (KUET), Bangladesh. This research work was also partially supported by the UGC funded research grants of KUET.

Disclosures

The authors declare no conflicts of interest.

References

1. B. Coleman, C. Coarsey, M. A. Kabir, and W. Asghar, "Point-of-care colorimetric analysis through smartphone video," Sens. Actuators B **282**, 225-231 (2019).
2. X. Li, F. Yang, J. X. H. Wong, and H. Z. Yu, "Integrated smartphone-app-chip system for on-site parts-per billion-level colorimetric quantitation of aflatoxins," Anal. Chem. **89**(17), 8908-8916 (2017).
3. P. Brangel, A. Sobarzo, C. Parolo, B. S. Miller, P. D. Howes, S. Gelkop, J. J. Lutwama, J. M. Dye, R. A. McKendry, L. Lobel, and M. M. Stevens, "A serological point-of-care test for the detection of IgG antibodies against Ebola virus in human survivors," ACS Nano **12**(1), 63-73 (2017).
4. Q. Wei, R. Nagi, K. Sadeghi, S. Feng, E. Yan, S. J. Ki, R. Caire, D. Tseng, and A. Ozcan, "Detection and spatial mapping of mercury contamination in water samples using a smart-phone," ACS Nano **8**(2), 1121-1129 (2014).
5. M. A. Hossain, J. Canning, S. Ast, P. Rutledge, T. L. Yen, and A. Jamalipour, "Lab-in-a-phone: smartphone-based portable fluorometer for pH measurements of environmental water," IEEE Sens. J. **15**(9), 5095-5102 (2015).
6. V. Kilic, G. Alankus, N. Horzum, A. Y. Mutlu, A. Bayram, and M. E. Solmaz, "Single-image-referenced colorimetric water quality detection using a smartphone," ACS Omega **3**(5), 5531-5536 (2018).
7. J. H. Lee, B. Fan, T. D. Samdin, D. A. Monteiro, M. S. Desai, O. Scheideler, H. E. Jin, S. Kim, and S. W. Lee, "Phage-based structural color sensors and their pattern recognition sensing system," ACS Nano **11**(4), 3632-3641 (2017).
8. T. H. Wu, C. C. Chang, J. Vaillant, A. Bruyant, and C. W. Lin, "DNA biosensor combining single-wavelength colorimetry and a digital lock-in amplifier within a smartphone," Lab Chip **16**(23), 4527-4533 (2016).
9. A. Y. Mutlu, V. Kılıç, G. K. Özdemir, A. Bayram, N. Horzum, and M. E. Solmaz, "Smartphone based colorimetric detection via machine learning," Analyst **142**(13), 2434-2441 (2017).
10. H. C. Wang, F. Y. Chang, T. M. Tsai, C. H. Chen, and Y. Y. Chen, "Development and clinical trial of a smartphone-based colorimetric detection system for self-monitoring of blood glucose," Biomed. Opt. Express **11**(4), 2166-2177 (2020).
11. H. Nguyen, I. Misbah, and W. C. Shih, "Smartphone nano-colorimetry for on-demand multiplex lead and mercury detection and quantitation in drinking water," IEEE Sens. J. **20**(12), 6685-6691 (2020).
12. W. Zhang, X. Niu, X. Li, Y. He, H. Song, Y. Peng, J. Pan, F. Qiu, H. Zhao, and M. Lan, "A smartphone-integrated ready-to-use paper-based sensor with mesoporous carbon-dispersed Pd nanoparticles as a highly active peroxidase mimic for H_2O_2 detection," Sens. Actuators B **265**, 412-420 (2018).
13. E. Guler, T. Y. Sengel, Z. P. Gumus, M. Arslan, H. Coskunol, S. Timur, and Y. Yagci, "Mobile phone sensing of cocaine in a lateral flow assay combined with a biomimetic material," Anal. Chem. **89**(18), 9629-9632 (2017).
14. D. Santra, S. Mandal, A. Santra, and U. K. Ghorai, "Cost effective and wireless portable device for estimation of hexavalent Chromium, Fluoride and Iron in drinking water," Anal. Chem. **90**(21), 12815-12823 (2018).

15. Y. Jung, J. Kim, O. Awofeso, H. Kim, F. Regnier, and E. Bae, "Smartphone-based colorimetric analysis for detection of saliva alcohol concentration," Appl. Opt. **54**(31), 9183-9189 (2015).
16. P. C. Biswas, S. Rani, M. A. Hossain, M. R. Islam, and J. Canning, "Multi-channel smartphone spectrometer using combined diffraction orders," IEEE Sens. Lett. **4**(9) (2020). DOI: 10.1109/LSENS.2020.3015590.
17. M. A. Hossain, J. Canning, K. Cook, and A. Jamalipour, "Optical fiber smartphone spectrometer," Opt. Lett. **41**(10), 2237-2240 (2016).
18. M. A. Hossain, J. Canning, S. Ast, K. Cook, P. J. Rutledge, and A. Jamalipour, "Combined "dual" absorption and fluorescence smartphone spectrometers," Opt. Lett. **40**(8), 1737-1740 (2015).
19. S. D. Kim, Y. Koo, and Y. Yun, "A smartphone-based automatic measurement method for colorimetric pH detection using a color adaptation algorithm," Sensors **17**(7), 1604-1616 (2017).
20. M.Y. Jia, Q. Wu, H. Li, Y. Zhang, Y. F. Guan, and L. Feng, "The calibration of cellphone camera-based colorimetric sensor array and its application in the determination of glucose in urine," Biosens. Bioelectron. **74**, 1029-1037 (2015).
21. T. C. Stubbings, and H. Hutter, "Combining multispectral image information using color," Anal. Chem. **72**(7), 282A-288A (2000).
22. A. F. Coskun, J. Wong, D. Khodadadi, R. Nagi, A. Teya, and A. Ozcan, "A personalized food allergen testing platform on a cellphone," Lab Chip **13**(4), 636-640 (2012).
23. S. Sumriddetchkajorn, K. Chaitavon, and Y. Intaravanne, "Mobile device-based self-referencing colorimeter for monitoring chlorine concentration in water," Sens. Actuators B **182**, 592-597 (2013).
24. L. Jiao, Z. Xu, W. Du, H. Li, and M. Yin, "Fast preparation of polydopamine nanoparticles catalyzed by Fe^{2+}/H_2O_2 for visible sensitive smartphone-enabled cytosensing," ACS Appl. Mater. Interfaces **9**(34), 28339-28345 (2017).
25. J. L. D. Nelis, Y. Zhao, L. Bura, K. Rafferty, C. T. Elliott, and K. Campbell, "A randomised combined channel approach for the quantification of colour and intensity based assays with smartphones," Anal. Chem. **92**(11), 7852-7860 (2020).
26. J. I. Hong and B. Y. Chang, "Development of the smartphone-based colorimetry for multi-analyte sensing arrays," Lab Chip 14(10), 1725-1732 (2014).
27. N. L. Ruiz, V. F. Curto, M. M. Erenas, F. B. Lopez, D. Diamond, A. J. Palma, and L. F. C. Vallvey, "Smartphone-based simultaneous pH and Nitrite colorimetric determination for paper microfluidic devices," Anal. Chem. **86**(19), 9554-9562 (2014).
28. A. Garcia, M. M. Erenar, E. D. Marinetto, C. A. Abad, I. D. Orbe-Paya, A. J. Palma, and L. F. C. Vallvey, "Mobile phone platform as portable chemical analyzer," Sens. Actuators B 156(1), 350-359 (2011).
29. S. Dutta, G. P. Saikia, D. J. Sarma, K. Gupta, P. Das, and P. Nath, "Protein, enzyme and carbohydrate quantification using smartphone through colorimetric digitization technique," J. Biophoton. **10**(5), 623-633 (2016).
30. V. Oncescu, D. O'Dell, and D. Erickson, "Smartphone based health accessory for colorimetric detection of biomarkers in sweat and saliva," Lab Chip **13**(16), 3232-3238 (2013).
31. U. M. Jalal, G. J. Jin, and J. S. Shim, "Paper-plastic hybrid microfluidic device for smartphone-based colorimetric analysis of urine," Anal. Chem. **89**(24), 13160-13166 (2017).
32. A. Motalebizadeh, H. Bagheri, S. Asiaei, N. Fekrat, and A. Afkhami, "New portable smartphone-based PDMS microfluidic kit for the simultaneous colorimetric detection of arsenic and mercury," RSC Adv. **8**(48), 27091-27100 (2018).
33. S. Rani, M. A. Hossain, P. C. Biswas, M. R. Islam, and J. Canning, "Multiple nonlinear regression-based adaptive colour model for smartphone colorimeter," in 14th Pacific Rim Conference on Lasers and Electro-Optics (CLEO PR 2020), OSA Technical Digest.
34. S. Sumriddetchkajorn, K. Chaitavon, and Y. Intaravanne, "Mobile-platform based colorimeter for monitoring chlorine concentration in water," Sens. Actuators B **191**, 561-566 (2013).
35. H. D. Cheng, X. H. Jiang, Y. Sun, and J. Wang, "Color image segmentation: advances and prospects," Pattern Recognition **34**(12), 2259-2281 (2001).
36. D. C. Montgomery, E. A. Peck, and G. G. Vining, "Introduction to linear regression analysis," Wily, Edition **5** (2012).